

# Numerical and Theoretical Investigation of the Scalar Dissipation Rate in Laminar Counterflowing Spray Flames

H. Olguin<sup>1,2</sup> and E. Gutheil<sup>1</sup>

<sup>1</sup>Interdisciplinary Center for Scientific Computing, University of Heidelberg, Germany

<sup>2</sup>Department of Mechanical Engineering, Universidad Técnica Federico Santa María, Chile

## 1 Introduction

The scalar dissipation rate  $\chi = 2D(\text{grad}\xi)^2$  of the mixture fraction,  $\xi$ , may be considered as the inverse characteristic diffusion time or the residence time in a flow, and it plays a dominant role in the modeling of combustion processes. In laminar counterflows, the scalar dissipation rate depends on the strain rate  $a$ , i.e. the velocity gradient of the gas velocity at a boundary of the counterflow configuration. As strain rate is increased in these flames, the residence time of the reactants is reduced and eventually, this continuous increase leads to flame extinction [1]. Thus, this characteristic variable plays an important role, for instance in the flamelet modeling of combustion processes, where the scalar dissipation rate at extinction characterizes the stability of flames [1].

During the last decades, transport equations for the scalar dissipation rate of the reaction progress variable or the mixture fraction have been derived for premixed [2, 3, 4, 5], non-premixed [6, 7] and for spray flames [8], respectively. Most often, chemical species are assumed to have the same diffusion coefficient, and Fick's diffusion law is adopted, which implies the negligence of effects associated with spatial variations of the mean molecular weight of the gas mixture,  $\bar{M}$ . For turbulent flames, research has focused on the averaging of the governing equations and on the modeling of unclosed terms. In this context, it is difficult to evaluate the accuracy of the equations and the validity of the assumptions involved, since errors are introduced in the models. Therefore, an evaluation of the equations in a simplified configuration is desirable.

Olguin and Gutheil [9] derived a transport equation for the scalar dissipation rate of the mixture fraction and validate it for counterflow spray flames. The present paper addresses the question which terms in the derived equation are important or negligible. For this purpose, the transport equation of the scalar dissipation rate of the mixture fraction [9] is solved for ethanol/air counterflow spray flames and evaluated, where both low and high strain rate situations are considered.

## 2 Derivation of the Exact Transport Equation for the Scalar Dissipation Rate of the Mixture Fraction

The main steps of the derivation of transport equations of the mixture fraction and its scalar dissipation rate are presented. A more detailed explanation is given by Olguin and Gutheil [9]. The transport

equation of the mass fraction  $Y_k$  of chemical species  $k$  yields

$$\rho \frac{\partial Y_k}{\partial t} + \rho u_i \frac{\partial Y_k}{\partial x_i} = \frac{\partial}{\partial x_i} \left( \rho D_k \frac{\partial Y_k}{\partial x_i} + \frac{D_T}{T} \frac{\partial T}{\partial x_i} \right) + \frac{\partial}{\partial x_i} \left( \rho \frac{D_k Y_k}{\bar{M}} \frac{\partial \bar{M}}{\partial x_i} \right) + \dot{\omega}_k + (\delta_{Fk} - Y_k) S_v, \quad (1)$$

where the Einstein summation convention is used,  $u_i$  is the gas velocity in  $i$  direction,  $\rho$  is the gas density, and  $S_v$  is a source of evaporated mass.  $\delta$  is the Kronecker symbol, the subscript  $F$  denotes fuel, and  $\dot{\omega}_k$  is the specific chemical reaction rate of species  $k$ ,  $k = 1, \dots, N$ .  $D_k$  is the diffusion coefficient of species  $k$  into the mixture,  $\bar{M}$  is the mean molecular weight of the mixture, and  $D_T$  is the thermal diffusion coefficient, which is considered for the light species H and H<sub>2</sub>. Multiplication of Eq. (1) with  $a_{Ck} M_C / M_k$  and summation over  $k = 1, \dots, N$  yields

$$\rho \frac{\partial \xi_C}{\partial t} + \rho u_i \frac{\partial \xi_C}{\partial x_i} = \frac{\partial}{\partial x_i} \left( \frac{M_F}{a_{CF}} \rho \sum_{k=1}^N \frac{a_{Ck}}{M_k} D_k \frac{\partial Y_k}{\partial x_i} \right) + \frac{\partial}{\partial x_i} \left( \frac{\rho M_F}{a_{CF} \bar{M}} \sum_{k=1}^N \frac{a_{Ck}}{M_k} D_k Y_k \frac{\partial \bar{M}}{\partial x_i} \right) + S_v (1 - \xi), \quad (2)$$

where the definitions of the carbon based mixture fraction,  $\xi_C = \frac{Z_C - Z_{C,\min}}{Z_{C,\max} - Z_{C,\min}}$ , and the carbon mass fraction,  $Z_C = \sum_{k=1}^N \left( \frac{a_{Ck} M_C}{M_k} \right) Y_k$ , have been employed.  $a_{kC}$  denotes the number of moles of carbon in species  $k$  and  $M_C$  and  $M_k$  denote the molecular weights of carbon and of species  $k$ , respectively. Using the assumption of equal molecular diffusion coefficients  $D_k = D$ , Eq. (2) can be rewritten as

$$\rho \frac{\partial \xi_C}{\partial t} + \rho u_i \frac{\partial \xi_C}{\partial x_i} = \frac{\partial}{\partial x_i} \left( \rho D \frac{\partial \xi_C}{\partial x_i} \right) + \frac{\partial}{\partial x_i} \left( \rho D \frac{\xi_C}{\bar{M}} \frac{\partial \bar{M}}{\partial x_i} \right) + S_v (1 - \xi). \quad (3)$$

In the remainder of the present work, the subscript C is omitted, and the mixture fraction is noted as  $\xi$ . Note that if Eq. (2) is to be equivalent to Eq. (3), the first and second terms of the r.h.s. of Eqs. (2) and (3) have to be equivalent, which leads to an expression for the optimum diffusion coefficient,  $D_o$

$$D_o = \frac{M_F \left( \sum_{k=1}^N \frac{a_{Ck}}{M_k} D_k \frac{\partial Y_k}{\partial x_i} + \frac{1}{\bar{M}} \sum_{k=1}^N \frac{a_{Ck}}{M_k} D_k Y_k \frac{\partial \bar{M}}{\partial x_i} \right)}{a_{CF} \left( \frac{\partial \xi}{\partial x_i} + \frac{\xi}{\bar{M}} \frac{\partial \bar{M}}{\partial x_i} \right)}. \quad (4)$$

Application of the operator  $\frac{\partial \xi}{\partial x_j} \frac{\partial}{\partial x_j}$  to each term in Eq. (3) leads to

$$\frac{\partial \chi}{\partial t} + u_i \frac{\partial \chi}{\partial x_i} = D \frac{\partial^2 \chi}{\partial x_i^2} + S_{\chi,g} + S_{\chi,v} + S_{\chi,\bar{M}}, \quad (5)$$

where the definition of  $\chi = 2D \left( \frac{\partial \xi}{\partial x_i} \right)^2$  was employed. The terms  $S_{\chi,g}$  and  $S_{\chi,v}$  in Eq. (5) account for sources stemming from the gas and the liquid phase, respectively, and the last term,  $S_{\chi,\bar{M}}$  accounts for variations of the mean molecular weight of the gas mixture. They yield

$$\begin{aligned} S_{\chi,g} = & -4D \frac{\partial \xi}{\partial x_i} \frac{\partial \xi}{\partial x_j} \frac{\partial u_j}{\partial x_i} - 4D^2 \left( \frac{\partial^2 \xi}{\partial x_i \partial x_j} \right)^2 - D \chi u_i \frac{\partial}{\partial x_i} \left( \frac{1}{D} \right) - \frac{4D}{\rho} \frac{\partial \xi}{\partial x_i} \frac{\partial \xi}{\partial x_j} u_i \frac{\partial \rho}{\partial x_j} \\ & + 2D^2 \frac{\partial \chi}{\partial x_i} \frac{\partial}{\partial x_i} \left( \frac{1}{D} \right) + \frac{4D}{\rho} \frac{\partial^2 \xi}{\partial x_i^2} \frac{\partial \xi}{\partial x_j} \frac{\partial (\rho D)}{\partial x_j} + \frac{4D}{\rho} \frac{\partial \xi}{\partial x_i} \frac{\partial}{\partial x_i} \left( \frac{\partial \xi}{\partial x_j} \frac{\partial (\rho D)}{\partial x_j} \right) \end{aligned} \quad (6)$$

$$- D \chi \frac{\partial}{\partial t} \left( \frac{1}{D} \right) - \frac{4D}{\rho} \frac{\partial \xi}{\partial t} \frac{\partial \xi}{\partial x_j} \frac{\partial \rho}{\partial x_j} + \chi D^2 \frac{\partial^2}{\partial x_i^2} \left( \frac{1}{D} \right),$$

$$S_{\chi,v} = \frac{4D}{\rho} \frac{\partial \xi}{\partial x_j} \frac{\partial}{\partial x_j} [S_v (1 - \xi)], \quad (7)$$

and

$$S_{\chi, \bar{M}} = \frac{D}{\bar{M}} \frac{\partial \bar{M}}{\partial x_i} \frac{\partial \chi}{\partial x_i} + \frac{4D\xi}{\rho} \frac{\partial \xi}{\partial x_i} \frac{\partial}{\partial x_i} \left[ \frac{\partial}{\partial x_j} \left( \frac{\rho D}{\bar{M}} \frac{\partial \bar{M}}{\partial x_j} \right) \right] + \frac{D^2 \chi}{\bar{M}} \frac{\partial \bar{M}}{\partial x_i} \frac{\partial}{\partial x_i} \left( \frac{1}{D} \right) \quad (8)$$

$$+ \frac{4D^2}{\bar{M}} \frac{\partial \xi}{\partial x_i} \frac{\partial \xi}{\partial x_j} \frac{\partial^2 \bar{M}}{\partial x_i \partial x_j} + \frac{4D}{\rho} \frac{\partial \bar{M}}{\partial x_i} \frac{\partial \xi}{\partial x_i} \frac{\partial \xi}{\partial x_j} \frac{\partial}{\partial x_j} \left( \frac{\rho D}{\bar{M}} \right) + \frac{2\chi}{\rho} \frac{\partial}{\partial x_i} \left( \frac{\rho D}{\bar{M}} \frac{\partial \bar{M}}{\partial x_i} \right). \quad (9)$$

If a mean molecular weight of the mixture is assumed, the terms including  $\partial \bar{M} / \partial x_i$  vanish, and the transport equations of  $\xi$  and  $\chi$  may be written as

$$\rho \frac{\partial \xi}{\partial t} + \rho u_i \frac{\partial \xi}{\partial x_i} = \frac{\partial}{\partial x_i} \left( \rho D \frac{\partial \xi}{\partial x_i} \right) + S_v(1 - \xi) \quad (10)$$

and

$$\frac{\partial \chi}{\partial t} + u_i \frac{\partial \chi}{\partial x_i} = D \frac{\partial^2 \chi}{\partial x_i^2} + S_{\chi, g} + S_{\chi, v}. \quad (11)$$

In the results' section, the following evaluation will be made. On the one hand, all species transport equations, Eqs. (1), will be solved, and the definition of the mixture fraction and its scalar dissipation rate will be evaluated. The results of this procedure will be denoted as  $\xi_e$  and  $\chi_e$  and compared with the direct solution of Eqs. (10) and (11) (denoted as  $\xi_t$  and  $\chi_t$ ) and of Eqs. (3) and (5) (denoted as  $\xi_{t,W}$  and  $\chi_{t,W}$ ). In all cases, a mass averaged diffusion coefficient of the mixture, i.e.  $D = \sum_{k=1}^N Y_k D_k$  will be employed. For the purpose of evaluating the above equations, numerical simulations of ethanol/air spray flames in the counterflow configuration are performed and analyzed [10, 11, 12, 13], where a detailed chemical reaction mechanism for ethanol/air at atmospheric pressure is used [14, 12].

### 3 Results and Discussion

Structures of mono-disperse laminar spray flames at low and high strain rates are presented and evaluated. In both cases, an ethanol spray carried by air is directed against an air flow in an axisymmetric counterflow configuration [9, 15]. The initial liquid and gas temperatures are 300 K, the initial gas and droplet velocities are  $v_g = v_l = 0.44$  m/s and the equivalence ratio is unity.

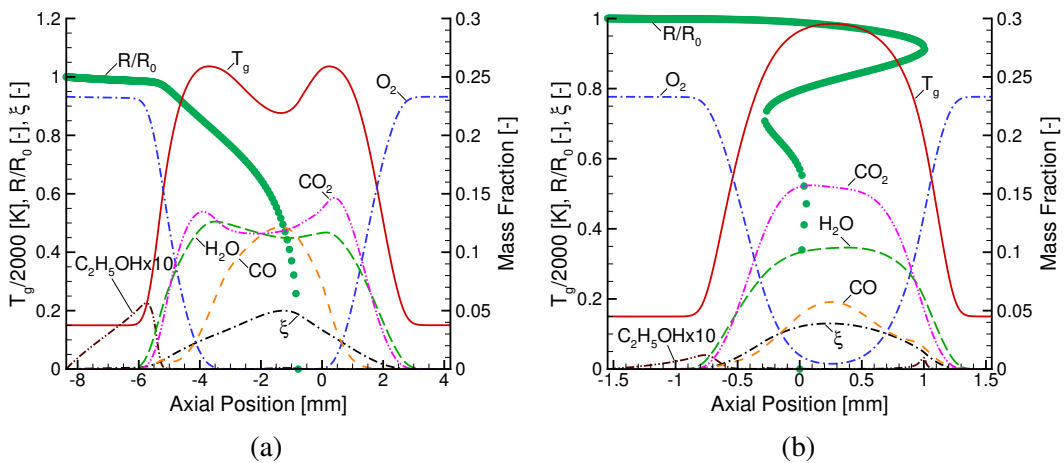


Figure 1: Outer ethanol/air flame structure,  $E = 1$ ,  $R_0 = 25 \mu\text{m}$ , (a)  $a = 55/s$ ; (b)  $a = 950/s$  [15].

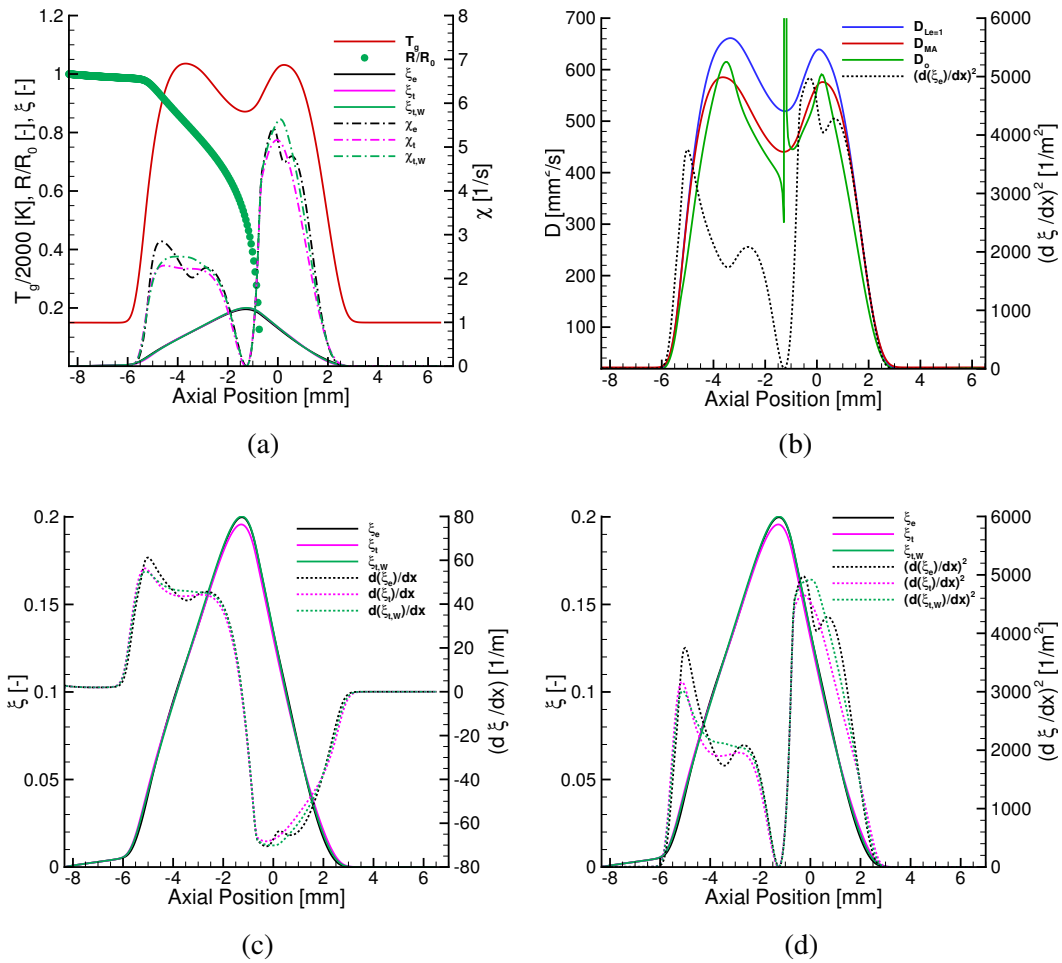


Figure 2: Profiles of (a)  $\chi$ ; (b)  $D$ ; (c)  $\frac{\partial \xi}{\partial x_i}$  and (d)  $\left(\frac{\partial \xi}{\partial x_i}\right)^2$ , for fixed  $a = 55/s$ .

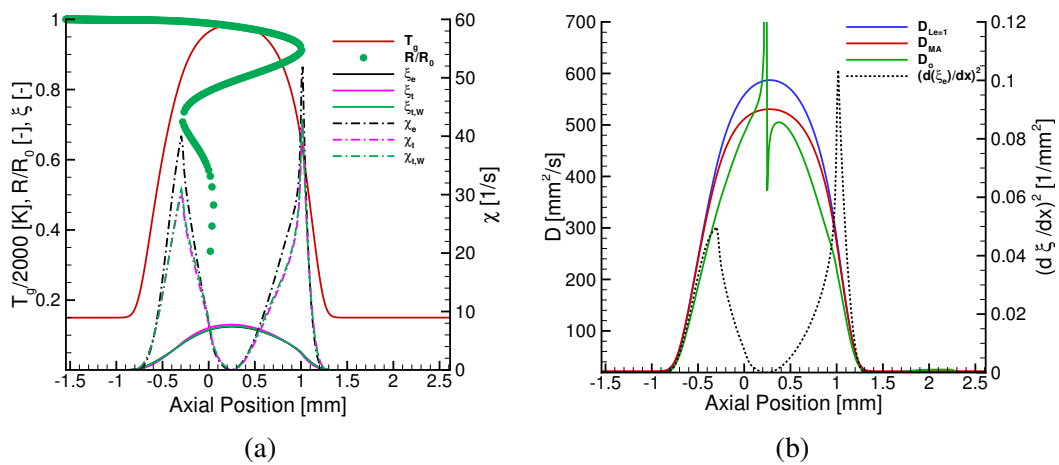


Figure 3: Profiles of (a)  $\chi$ ; (b)  $D$ ,  $a = 950/s$

Figure 1 (a) shows the outer flame structure for 55/s. Here, droplets are completely evaporated before they reach the stagnation plane located at the axial position  $x = 0$  mm, and two reaction zones are found which are separated by a low temperature region [12]. For the high strain rate situation (Fig. 1 (b)), the droplets cross the stagnation plane, reverse their motion and start to oscillate around  $x = 0$ , which leads to a locally poly-disperse flame structure, even when the boundary conditions are mono-disperse. Under these conditions, the two reaction zones merge and a single peak in gas temperature is found. Structures presented in Fig. 1 have already been discussed in a different context in previous work, and the reader is referred to [9, 15, 12] for a complete analysis.

Figure 2 (a) shows profiles of  $\xi_e$ ,  $\xi_t$  as well as  $\xi_{t,W}$  and  $\chi_e$ ,  $\chi_t$  and  $\chi_{t,W}$  for low strain rate. In the case of the mixture fraction, only small differences between the different profiles are found, which confirms that terms associated with  $\frac{\partial \bar{M}}{\partial x}$  are not important for the profiles of mixture fraction. Thus, Eq. (10) is an excellent approximation [9]. However, the comparison of the profiles of the scalar dissipation rate reveals bigger differences, since gradients of mixture fraction are involved in the definition of  $\chi$ , leading to a higher sensitivity compared with  $\xi$ . Although the inclusion of effects associated with spatial variations of the mean molecular weight tends to improve the prediction of  $\chi$  somewhat, both formulations, with and without terms containing  $\frac{\partial \bar{M}}{\partial x}$ , do not properly predict the peak values of  $\chi$ . Figure 2 (b) shows profiles of the diffusion coefficients employing the assumption of unity Lewis number, a mass averaged diffusion coefficient and the optimum value calculated using Eq. (4). It is clear that the use of a mass averaged diffusion coefficient is better than the assumption of unity Lewis number, although there is still space for improvement. The small errors in the predicted values of  $\xi$  increase for the gradient and the square of the gradient illustrated in Figs. 2 (c) and (d). This leads to the large differences observed between the predicted and expected profiles of  $\xi$  displayed in Fig. 2 (a).

Figure 3 (a) shows corresponding profiles of  $\xi$  and  $\chi$  for a strain rate of 950/s. It can be seen that under these conditions, Eqs. (10) and (11) are both excellent approximations, which implies that terms including  $\frac{\partial \bar{M}}{\partial x}$  are negligibly small and that the consideration of Fick's diffusion law at high strain rate situations is justified. Figure 3 (b) clearly shows that also for this case, the mass averaged diffusion coefficient considerably differs from  $D_o$ . These results support the conclusion that differences between predicted ( $\chi_t$  and  $\chi_{t,W}$ ) and expected values ( $\chi_e$ ) are due to the inadequacy of the diffusion coefficient selected for  $\chi$  and not to the use of Fick's diffusion law.

## 4 Conclusions

The scalar dissipation rate transport equation derived by Olguin and Gutheil [9] is solved with and without considering terms associated with spatial variations of the mean molecular weight of the mixture  $\bar{M}$ . Laminar ethanol/air counterflow spray flames in the counterflow configuration at low and high strain rate are considered. The results are compared with the exact value of the scalar dissipation rate obtained by means of the resolution of all chemical species transport equations (Eq. (1)) and use of the definition of  $\chi$ . It is found that Fick's diffusion law is appropriate for high strain rate situations and that differences between calculated and expected values of  $\chi$  are not due to the negligence of effects associate with  $\frac{\partial \bar{M}}{\partial x_i}$ , but to the inadequacy of the selected diffusion coefficient of the mixture.

## Acknowledgments

H.O. thanks the DAAD for financial support through a research fellowship. Financial support of the German Science Foundation through the Heidelberg Graduate School of Mathematical and Computational Methods for the Sciences "MathComp" of IWR is gratefully acknowledged.

**References**

- [1] Peters, N. (1984). Laminar diffusion flamelet models in non-premixed turbulent combustion. *Prog. Energy Combust. Sci.* 10: 319
- [2] Mantel, T. and Borghi, R. (1994). A new model of premixed wrinkled flame propagation based on a scalar dissipation equation. *Combust. Flame* 96: 443
- [3] Mura, A. and Borghi, R. (2003). Towards an extended scalar dissipation equation for turbulent premixed combustion. *Combust. Flame* 133: 193
- [4] Mura, A., Robin, V. and Champion, M. (2007). Modeling of scalar dissipation in partially premixed turbulent flames. *Combust. Flame* 149: 217
- [5] Dunstan, T., Minamoto, Y., Chakraborty, N. and Swaminathan, N. (2013). Scalar dissipation rate modelling for Large Eddy Simulation of turbulent premixed flames. *Proc. Combust. Inst.* 34: 1193
- [6] Cha, C. M., Kosaly, G. and Pitsch, H. (2001). Modeling extinction and reignition in turbulent nonpremixed combustion using a doubly-conditional moment closure approach. *Phys. Fluids* 13: 3824
- [7] Pitsch, H., Cha, C. M. and Fedotov, S. (2003). Flamelet modelling of non-premixed turbulent combustion with local extinction and re-ignition. *Combust. Theory Model.* 7: 317
- [8] Gomet, L., Robin, V. and Mura, A. (2014). Lagrangian modelling of turbulent spray combustion under liquid rocket engine conditions. *Acta Astronaut.* 94: 184
- [9] Olguin, H. and Gutheil, E. (2014). Derivation and evaluation of a multi-regime spray flamelet model. *Z. Phys. Chem*, DOI: 10.1515/zpch-2014-0572
- [10] Continillo, G. and Sirignano, W.A. (1990). Counterflow spray combustion modeling. *Combust. Flame* 81: 325
- [11] Gutheil, E. and Sirignano, W.A. (1998). Counterflow spray combustion modeling with detailed transport and detailed chemistry. *Combust. Flame* 113: 92
- [12] Gutheil, E. (2001). Structure and extinction of laminar ethanol-air spray flames. *Combust. Theory Model.* 5: 1
- [13] Gutheil, E. (2005). Multiple solutions for structures of laminar counterflow spray flames. *Prog. Comput. Fluid Dyn.* 5: 414
- [14] Chevalier, C. (1993). Entwicklung eines detaillierten Reaktionsmechanismus zur Modellierung der Verbrennungsprozesse von Kohlenwasserstoffen bei Hoch- und Niedertemperaturbedingungen. PhD Thesis, Universität Stuttgart, Germany (in German)
- [15] Olguin, H. and Gutheil, E. (2014). Influence of evaporation on spray flamelet structures. *Combust. Flame* 161: 987